Ferroelectric Phase Transition in LiNbO$_3$: Insights From Molecular Dynamics

Simone Sanna and Wolf Gero Schmidt

Abstract—*Ab initio* molecular dynamics within density functional theory is used for the first time to model the ferroelectric–paraelectric phase transition in LiNbO$_3$. Our calculations show that the structural phase transition is not an abrupt event, but rather a continuous process occurring over a range of about 100K and involving different ionic species at different temperatures. Because of the different behavior of the Li and Nb sublattices, the ferroelectric transition displays both displacive and order–disorder character.

I. Introduction

LITHIUM niobate is one of the most important optical materials; in the fields of optics, nonlinear optics, and optoelectronics, it plays the role played by silicon in standard electronics. LiNbO$_3$ crystals have unique and favorable ferroelectric, piezoelectric, photoelastic, optical (linear and nonlinear), and electro-optical properties; furthermore, they are strongly birefringent [1]. Because of its properties, LiNbO$_3$ is used extensively for applications such as optical waveguides, optical switchers, acousto-optical devices, and lasers, as well as in widespread devices such as motion controllers and mobile telephones.

Despite this wide range of applications, many aspects of the physics underlying the LiNbO$_3$ properties are not yet fully understood. In particular, the phase transition between the paraelectric and the ferroelectric phase is still the subject of debate. A major point concerning the nature of the transition is whether it is of the displacive or order–disorder type. Displacive transitions are typically characterized by the presence of a polar optical phonon mode, which becomes soft close to the Curie temperature, θ_C. On the contrary, no soft mode exists in order–disorder transitions, because of the presence of a double-well potential with a barrier much larger than the thermal energy, $k_B\theta_C$. Many different studies have been dedicated to the investigation of the phonon modes of LiNbO$_3$. Unfortunately only some of the investigations, including Rayleigh scattering, Raman spectroscopy, and infrared reflectivity, show a soft-mode behavior for an A_1 (TO) optical phonon, suggesting a displacive nature of the transition [2]–[4]; in other studies, including neutron and Raman scattering experiments, no mode softening could be observed, suggesting the order–disorder nature of the ferroelectric phase transition [5]–[7]. Wood *et al.* measured

the birefringence of lithium niobate tantalate crystals for various compositions and temperatures, finding that it changes continuously across the Curie temperature [8]. Theoretical investigations based on the modeling of the phonon modes within the frozen phonon approach support an order–disorder model for the oxygen atoms as the driving mechanism for the ferroelectric instability [9], [10]. Recently, Phillpot and Gopalan used molecular dynamics within the shell-model as proposed by Tomlinson *et al.* [11] to characterize the ferroelectric phase transition, showing coupled displacive and order–disorder dynamics [12]. Lee *et al.* performed similar calculations to validate their approach, to be used for the investigation of the domain walls in LiNbO$_3$ [13]. Here, the interatomic interactions were modeled by a Jackson potential [14]. Even if both the Tomlinson and the Jackson potential reproduce the basic properties of LiNbO$_3$ to a satisfactory degree, they predict a different behavior of the Nb sublattice below the Curie temperature.

The high-temperature phase of LiNbO$_3$ (above 1483K) is paraelectric and belongs to the space group $R\bar{3}c$. According to the general understanding of this structure, the Li ions lie (at least in average) in the oxygen plane, whereas the Nb atoms are located at the centers of octahedral oxygen cages, as shown in Fig. 1 (central picture). When the temperature drops below the Curie temperature θ_C, the cations are displaced along the c-axis from their (high symmetry) sites; Nb ions are no longer at the center of the oxygen cages and the Li atoms sit either above or below the oxygen layers. Because of the Coulomb repulsion, both cations are displaced in the same direction with respect to the oxygen sublattice, as shown in Fig. 1 (left and right sides). This atomic rearrangement has two important consequences: First, the crystal loses the inversion symmetry and becomes noncentrosymmetric (space group $R3c$). Second, the center of mass of the positive and negative charges are displaced, giving rise to a spontaneous polarization along the c-axis as large as 0.7 C/m^2.

In this work, we perform molecular dynamics (MD) simulations to model the transition between the two phases and understand the mechanisms of the transition itself. To our knowledge, MD simulations in the framework of the density functional theory (DFT) are used here for the first time to gain insight into the transition dynamics.

II. Methods

Our first-principles calculations within the density functional theory (DFT) use the all-electron projector-
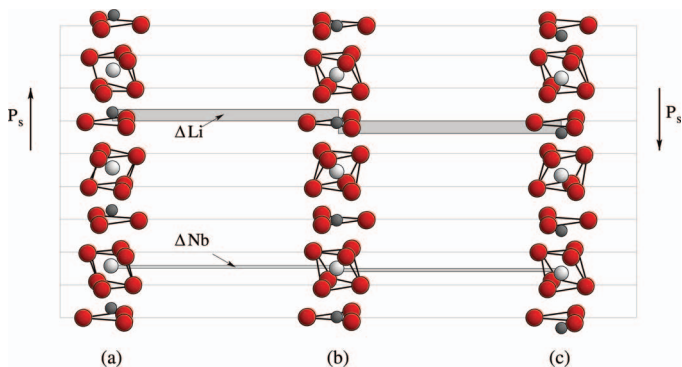
Fig. 1. Atomic structure of the (a) and (c) ferroelectric and (b) paraelectric phase of LiNbO$_3$. The displacement of the Nb atoms (in white) from their positions in the paraelectric phase is labeled by ΔNb, whereas the displacement of the Li ions (in gray) from the oxygen planes is labeled by ΔLi. Both displacements occur along the crystal c-axis.

augmented wave (PAW) method [15] as implemented in VASP [16]. The PW91 formulation of the generalized gradient approximation (GGA) exchange-correlation functional [17], plane wave expansions up to 400 eV, and projectors up to $l = 3$ for Nb and $l = 2$ for Li and O have been used for the calculations. A Monkhorst–Pack (MP) $6 \times 6 \times 6$ k-point mesh [18] was used to carry out the integration in the Brillouin zone for the simulation of the crystal structure. This approach yields reliable structures and energies for bulk LiNbO$_3$ in the ferroelectric and paraelectric phase and LiNbO$_3$ surfaces [19]–[21]. Minimizing the interatomic forces under a threshold value of 0.01 eV/Å and the total energy, we find lattice parameters $a = 5.161$ Å, $c = 13.902$ Å for the ferroelectric and $a = 5.342$ Å, $c = 13.589$ Å for the paraelectric structures, which are, in both cases, about 1% larger than the experimental values [1], [22]. The internal parameters are also fully relaxed. The calculated displacements of the Nb ions from the oxygen cage center (previously called ΔNb) and of the Li ions from the oxygen planes (ΔLi) in the ferroelectric phase are 0.28 and 0.72 Å, respectively. The density functional theory is a ground-state theory, which, in its customary formulation, is only valid for vanishing temperatures. To model atomic systems at finite temperatures, molecular dynamics calculations can be performed. In this approach, the investigated system is coupled with a thermostat, which initializes the velocities of the ions according to the Maxwell–Boltzmann distribution at the given temperature. The time evolution of the system is then modeled by solving the Newtonian equation of motion by means of a Verlet algorithm. This allows the system to be modeled at different temperatures and to consider anharmonicity effects, thus making the simulation of annealing and cooling-down processes, or even of temperature-driven phase transitions, possible. In our work, molecular dynamics calculations are performed within a supercell consisting of a $2 \times 2 \times 2$ repetition of the unit cell (i.e., 80 atoms) and $2 \times 2 \times 2$ MP k-point mesh. MD runs of about 5 ps starting with the structure in the ferroelectric phase and for temperatures of 500K, 750K, 1000K, 1250K, and 1500K are

performed, coupling the system to the Nosé thermostat [23]. Note that in the DFT-MD, the interatomic interactions are calculated at each step from first principles, i.e., no measured or fitted parameters, which would limit the predictive power of the method, enter into the calculation.

III. RESULTS AND DISCUSSION

To investigate the dynamics of the phase transition, we perform several MD runs at different temperatures and study the evolution of the parameters ΔLi and ΔNb, which measure the structural differences between the two LiNbO$_3$ phases. Above the Curie temperature, ΔLi and ΔNb are expected to be, at least on average, exactly zero, whereas at 0K they assume the calculated values of 0.28 and 0.72 Å, respectively. In Fig. 2, we show a Gaussian fit of the probability distribution of ΔLi at different temperatures. The curve representing the distribution at 500K is unimodal, suggesting that all of the Li ions are placed above the oxygen planes, as is expected for the system in the ferroelectric phase.

The fact that the calculated curves are perfectly fitted by one (or more) Gaussian functions suggests that the form of the distribution is due to a thermal broadening around a mean value. This mean value, centered around 0.74 Å, is slightly larger than the calculated value (at 0K) and in qualitative agreement with the measured value at room temperature. The curve at 1500K, i.e., above the transition phase, changes drastically. The distribution is now bimodal and symmetric with respect to ΔLi = 0, indicating that in the paraelectric phase most of the Li atoms lie either above or below the oxygen planes and only a small fraction lie exactly in the plane. The spontaneous
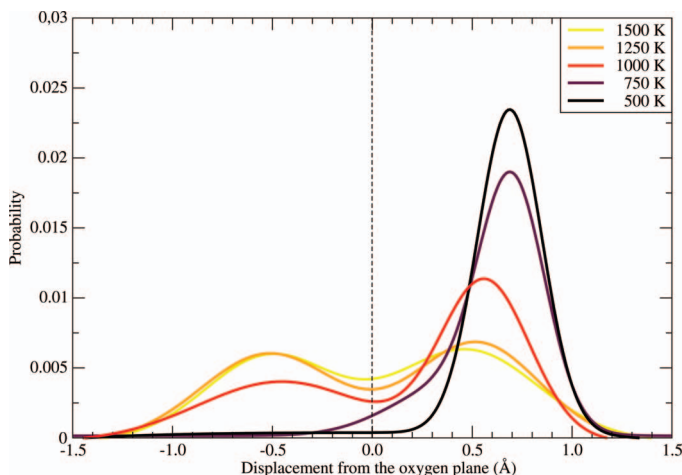

Fig. 2. Probability distribution of the parameter ΔLi (representing the displacement of the Li ions from the oxygen planes) at different temperatures. The unimodal distribution at 500K (well below the Curie temperature) means that all of the Li ions are located above the oxygen planes, whereas the symmetric bimodal curve at 1500K (above the Curie temperature) indicates that the Li ions are randomly distributed above or below the oxygen planes, as expected for an order–disorder phase transition.
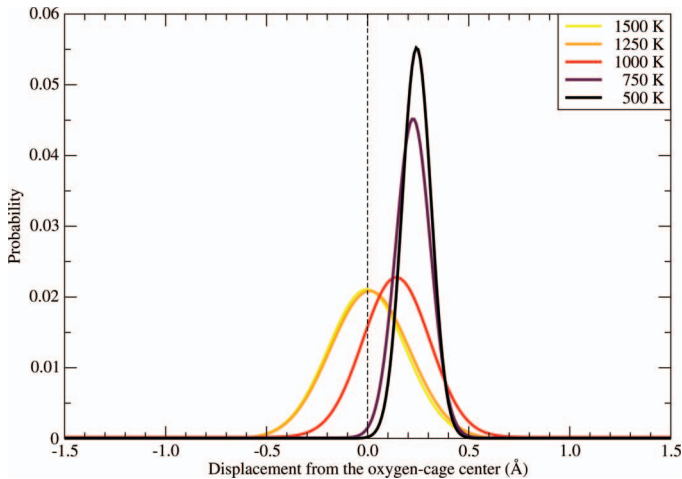
Fig. 3. Probability distribution of the parameter ΔNb (representing the displacement of the Nb ions from the center of the oxygen cages) at different temperatures. The distribution becomes broader at higher temperatures but remains unimodal, as expected for a displacive phase transition. Note that at 1000K, i.e., well below the Curie temperature, the Nb ions are already quite close to the center of the oxygen cages, indicating that the phase transition starts for the Nb sublattice at temperatures lower than θ_C.

polarization of the material will therefore be exactly zero only in average, because each unit cell is characterized by a finite, randomly distributed, polarization value. This feature is in agreement with an order–disorder character of the transition.

The small fraction of Li sitting in the oxygen planes suggests that it represents a higher energy lattice site than the site occupied in the ferroelectric phase, i.e., an energetic barrier. All other curves (temperature between 750K and 1250K) are between the two described distributions, meaning that with increasing temperature a growing fraction of Li atoms will posses enough thermal energy to pass this barrier. At 1500K, all Li atoms have sufficient energy to move across the plane, so that they can be found with the same probability over or under an oxygen plane, and the total Li contribution to the polarization vanishes. We observe that at temperatures substantially lower than θ_C an important fraction of the Li atoms is already no longer in the lattice site occupied in the ferroelectric phase. This suggests that the phase transition does not occur abruptly at a given temperature, but is rather a continuous process, occurring dynamically over a certain range of temperatures.

In Fig. 3, we show the Gaussian fit of the probability distribution of ΔNb at different temperatures. In contrast to the ΔLi probability, the distribution is unimodal at each investigated temperature, as expected for a displacive transition. This also suggests that, in contrast to the Li sublattice, the Nb sublattice does not need to overcome an energy barrier to move from the ferroelectric to the paraelectric configuration. At 500K, the distribution is centered about 0.29 Å, again slightly larger than the calculated value (at 0K) and in qualitative agreement with the measured value. At higher temperatures, the mean

value of the distribution moves toward ΔNb $= 0$, i.e., the Nb atoms move toward the center of the oxygen cages. For temperatures around 1000K, the Nb ions are already close to the cage centers and at 1250K they are exactly in their paraelectric lattice site. At higher temperatures, the distribution becomes broader, as the atoms vibrate with larger amplitude around their equilibrium positions. This behavior is in agreement with the prediction of Phillpot and Gopalan [12], whereas it differs from the results of [13], in which the Nb displacement was found not to vanish until the Curie temperature.

Our calculations confirm the suggestion first made in [12] that the phase transition is a two-step process involving a displacive transition of the Nb ions in the oxygen octahedral cages at a temperature below θ_C and an order–disorder transition in the Li–O planes, which is completed at θ_C. The atomic structure and the spontaneous polarization change gradually between the two phases, so that the transition does not occur at a well-defined temperature, but rather over a temperature range of more than 100K.

IV. Conclusion

We have performed *ab initio* MD simulations to investigate the nature of the ferroelectric–paraelectric transition in stoichiometric LiNbO$_3$. As for other ferroelectrics, the structural transition in LiNbO$_3$ can be thought of as being of a displacive nature far from the transition temperature and as showing order–disorder characteristics close to the Curie temperature θ_C. Furthermore, our calculations reveal that the paraelectric phase must be thought of as a random distribution of Li ions above and below the oxygen planes (with a nonzero value of ΔLi for most Li ions) and with an average zero net polarization, rather than in the commonly accepted configuration shown in Fig. 1(b).

References

[1] R. S. Weis and T. K. Gaylord, "Lithium niobate: Summary of physical properties and crystal structure," *Appl. Phys. A*, vol. 37, no. 4, pp. 191–203, 1985.
[2] A. S. Barker, Jr. and R. Loudon, "Dielectric properties and optical phonons in LiNbO$_3$," *Phys. Rev.*, vol. 158, no. 2, pp. 433–445, 1967.
[3] W. D. Johnston, Jr. and I. P. Kaminow, "Temperature dependence of Raman and Rayleigh scattering in LiNbO$_3$ and LiTaO$_3$," *Phys. Rev.*, vol. 168, no. 3, pp. 1045–1054, 1968.
[4] J. L. Servoin and F. Gervais, "Soft vibrational mode in LiNbO$_3$ and LiTaO$_3$," *Solid State Commun.*, vol. 31, no. 5, pp. 387–391, 1979.
[5] M. R. Chowdhury, G. E. Peckham, R. T. Ross, and D. H. Saunderson, "Lattice dynamics of lithium niobate," *J. Phys. C*, vol. 7, no. 6, pp. L99–L102, 1974.
[6] S. Koijima, "Order–disorder nature of ferroelectric phase transition in stoichiometric LiNbO$_3$ crystals," *Ferroelectrics*, vol. 223, no. 1, pp. 63–70, 1999.

[7] A. F. Penna, A. Chaves, P. Andrade, and S. P. S. Porto, "Light scattering by lithium tantalate at room temperature," *Phys. Rev. B*, vol. 13, no. 11, pp. 4907–4917, 1976.

[8] I. J. Wood, P. Daniels, R. H. Brown, and A. M. Glazer, "Optical birefringence study of the ferroelectric phase transition in lithium niobate tantalate mixed crystals: $LiNb_{1-x}Ta_xO_3$," *J. Phys. Condens. Matter*, vol. 20, no. 23, art. no. 235237, 2008.

[9] I. Inbar and R. E. Cohen, "Comparison of the electronic structures and energetics of ferroelectric $LiNbO_3$ and $LiTaO_3$," *Phys. Rev. B*, vol. 53, no. 3, pp. 1193–1204, 1996.

[10] J. Yu and K. Park, "First principles total energy study of ferroelectric transitions in $LiNbO_3$," *Physica B*, vol. 237–238, no. 1, pp. 341–344, 1997.

[11] S. M. Tomlinson, C. V. Freeman, C. R. A. Catlow, H. Donnerberg, and M. Leslie, "Atomistic simulation studies of technologically important oxides," *J. Chem. Soc., Faraday Trans. II*, vol. 85, no. 5, pp. 367–383, 1989.

[12] S. R. Phillpot and V. Gopalan, "Coupled displacive and order–disorder dynamics in $LiNbO_3$ by molecular-dynamics simulation," *Appl. Phys. Lett.*, vol. 84, no. 11, pp. 1916–1918, 2004.

[13] D. Lee, H. Xu, V. Dierolf, V. Gopalan, and S. R. Phillpot, "Structure and energetics of ferroelectric domain walls in $LiNbO_3$ from atomic-level simulations," *Phys. Rev. B*, vol. 82, no. 1, art. no. 014104, 2010.

[14] R. A. Jackson and M. E. G. Valerio, "A new interatomic potential for the ferroelectric and paraelectric phases of $LiNbO_3$," *J. Phys. Condens. Matter*, vol. 17, no. 6, pp. 837–843, 2005.

[15] P. E. Blöchl, "Projector augmented-wave method," *Phys. Rev. B*, vol. 50, no. 24, p. 17953–17979, 1994.

[16] G. Kresse and J. Furthmüller, "Efficient iterative schemes for *ab initio* total-energy calculations using a plane-wave basis set," *Phys. Rev. B*, vol. 54, no. 16, pp. 11169–11186, 1996.

[17] J. P. Perdew and Y. Wang, "Accurate and simple density functional for the electronic exchange energy: Generalized gradient approximation," *Phys. Rev. B*, vol. 33, no. 12, pp. 8800–8802, 1986.

[18] H. J. Monkhorst and J. D. Pack, "Special points for Brillouin-zone integrations," *Phys. Rev. B*, vol. 13, no. 12, pp. 5188–5192, 1976.

[19] W. G. Schmidt, M. Albrecht, S. Wippermann, S. Blankenburg, E. Rauls, F. Fuchs, C. Rödl, J. Furthmüller, and A. Hermann, "$LiNbO_3$ ground- and excited-state properties from first-principles calculations," *Phys. Rev. B*, vol. 77, no. 3, art. no. 035106, 2008.

[20] C. Thierfelder, S. Sanna, A. Schindlmayr, and W. G. Schmidt, "Do we know the band gap of lithium niobate?" *Phys. Status Solidi C*, vol. 7, no. 2, pp. 362–365, 2010.

[21] S. Sanna and W. G. Schmidt, "Lithium niobate X-cut, Y-cut, and Z-cut surfaces from *ab initio* theory," *Phys. Rev. B*, vol. 81, no. 21, art. no. 214116, 2010.

[22] H. Boysen and F. Altorfer, "A neutron powder investigation of the high-temperature structure and phase transition in $LiNbO_3$," *Acta Crystallogr. B*, vol. B50, no. 4, pp. 405–414, 1994.

[23] S. Nosé, "A unified formulation of the constant temperature molecular dynamics methods," *J. Chem. Phys.*, vol. 81, no. 1, pp. 511–519, 1984.

Simone Sanna was born in Cagliari, Italy, in 1977. He graduated in physics in 2003 and received his Ph.D. degree in physics in 2007. Since then, he has been a postdoctoral fellow at Paderborn University. His research interests are ferroelectrics and point defects.

Wolf Gero Schmidt was born in 1968. He studied physics in Jena, Germany. He graduated in physics in 1993 and received his Ph.D. degree in 1997. Since 2006, he has been a full professor of theoretical physics at Paderborn University. His research interests are the physics and chemistry of surfaces and interfaces, nanoscale science, and computational physics.